

Received 4 November 2023, accepted 7 December 2023, date of publication 18 December 2023,  
date of current version 29 December 2023.

Digital Object Identifier 10.1109/ACCESS.2023.3343770

## RESEARCH ARTICLE

# Combined MPC and Dynamic Neural Network-Based UAVs Trajectory Tracking Control

LEI YANG<sup>1</sup>, LIGANG WU<sup>2</sup>, YUANYUAN LV<sup>3</sup>, AND ZHE ZHANG<sup>3</sup>

<sup>1</sup>College of Physical and Electronic Sciences, Shanxi Datong University, Datong 037009, China

<sup>2</sup>College of Mechanical and Electrical Engineering, Shanxi Datong University, Datong 037009, China

<sup>3</sup>College of Coal Engineering, Shanxi Datong University, Datong 037009, China

Corresponding author: Ligang Wu (ligangwu@yeah.net)

This work was supported in part by the Project of Science and Technology Innovation of Higher Education Institutions in Shanxi Province under Grant 2022L436, in part by the Project of Scientific Research Fund of Shanxi Datong University under Grant 2020CXZ2, and in part by the Shanxi Datong University Teaching Reform Innovation Project under Grant XJG2022269.

**ABSTRACT** This paper focuses on the trajectory tracking problem of unmanned aerial vehicles (UAVs) under external disturbances, and a trajectory tracking method that combines model predictive control with dynamic neural networks was proposed. Firstly, the trajectory tracking problem is transformed into a constrained quadratic programming problem using the idea of model predictive control. Then, the kinematic constraints are taken into account, and control increment constraints and relaxation factors are designed in the objective function. A dynamic neural network is introduced to solve this quadratic programming problem in real-time. In addition, a disturbance compensation observer is designed to overcome external disturbances. Finally, numerical simulations are conducted to verify that the proposed tracking strategy reduces computational

**INDEX TERMS** External disturbances, trajectory tracking, dynamic neural networks, model predictive control.

## I. INTRODUCTION

Unmanned aerial vehicles (UAVs) play a crucial role in search and rescue research, such as fire monitoring [1] and assisting in rescue operations [2]. With an increasing number of UAVs being deployed in practical applications, scholars have conducted extensive research on their motion control [3], [4]. Due to the diverse mission requirements and the UAV's maneuverability, it is essential for it to accurately track the desired trajectory under external disturbances [5]. Therefore, this paper focuses on the study of UAV trajectory tracking control in the presence of external disturbances.

In recent years, numerous trajectory tracking control algorithms for UAVs have emerged. Methods such as proportional/integral/derivative control, back stepping, disturbance observer, and adaptive control have been proposed in [6],

[7], and [8]. Back stepping, which is based on Lyapunov theory and designed in a forward-backward recursive manner, is one of these methods. In [9] utilized integral back stepping to achieve trajectory tracking for a single UAV. In [10], on the other hand, designed a control algorithm based on back stepping to achieve trajectory tracking for a time-varying formation of multiple UAVs. Sliding mode control aims to drive the state of the controlled system onto a predefined sliding surface and maintain motion on the surface. It is effective in addressing model uncertainties and achieving trajectory tracking control. In [11] employed sliding mode control to achieve position and attitude control for a single UAV. The stability was proven using Lyapunov theory, and the effectiveness of the proposed approach was verified through simulations. In [12] proposed a combined approach using back stepping and sliding mode control and proved the stability of a single UAV system under the proposed algorithm using Lyapunov stability theory. As multirotor

The associate editor coordinating the review of this manuscript and approving it for publication was Xiwang Dong.

UAVs are often deployed in environments with significant external disturbances, there is a high requirement for control accuracy.

However, due to certain limitations in individual UAV during mission execution, research on multi-UAV cooperative control has become increasingly important. Multi-UAV cooperative formation control is an important technique in autonomous cooperative control methods for multiple UAVs, which enables the use of multiple UAVs to accomplish complex tasks such as coordinated search, disaster area rescue, commercial performances, etc.

Currently, there have been significant achievements in multi-UAV trajectory tracking, such as, an efficient control schemes based on onboard commodity sensors are presented for autonomous UAVs in indoor applications, where the horizontal displacement of the platform is provided by an optical flow sensor [13] address the trajectory tracking control (i.e., outer-loop control) problem for UAVs in the presence of modeling uncertainties and external disturbances. In [14] study trajectory tracking control of thrust-vectoring UAV and a geometric approach to the trajectory tracking control of UAVs with thrust vectoring capabilities is proposed. In [15] address the trajectory tracking problem for VTOL UAVs in which the thrust vector can be delivered only in a fixed direction with respect to the aircraft frame. In [16] consider a collaborative tracking control problem using a group of fixed-wing unmanned aerial vehicles with constant and non-identical speeds.

A framework for autonomous waypoint planning, trajectory generation through waypoints, and trajectory tracking for UAVs is proposed in [17]. The total energy use of the vehicle can be reduced and the control performance can be improved by appropriately considering the pitch angle of the vehicle in varying flight conditions was designed in [18]. In [19] present a review of high-angle-of-attack aerodynamic models as well as an algorithm for finding the optimal pitch and thrust of a winged eVTOL throughout its flight regime. Theoretical analysis and numerical simulation results show that the model has the fast convergence, high control accuracy, strong stability and good robustness is designed in [20]. Recently proposed control methods, suitable for trajectory tracking in fully actuated UAVs, are reviewed and experimentally compared in [21]. A robust adaptive formation and trajectory tracking control of multiple quad-rotor UAVs using super twisting sliding mode control method was proposed in [22].

Although significant progress has been made in the research of UAVs, there are still many underlying issues that need to be addressed. Firstly, the tracking system models of UAVs are coupled and nonlinear [23], making UAV tracking difficult to control and potentially leading to collision accidents in worst-case scenarios. In this regard, [24] proposed a cooperative path tracking controller for UAVs considering constant disturbances and time-varying delays. The second issue is the presence of complex external disturbances, which

can further impose constraints and result in tracking failures. This paper establishes a nonlinear tracking system model for UAVs and investigates the problem of UAV trajectory tracking under the influence of complex external disturbances, which presents certain challenges.

The major contributions of this study, which distinguish from the related literatures, are summarized as follows.

1. Compared to some existing research works on multi-UAV trajectory tracking [20], [22], our work establishes a discrete model for UAVs and addresses the issue of control variable coupling, making it more aligned with the practical engineering scenarios.

2. Considering the constraints of UAV kinematics, we design control increment constraints and relaxation factors in the objective function, and introduce a dynamic neural network to solve the model predictive control-based quadratic programming problem in real-time. Additionally, we design disturbance compensation observers to overcome disturbances. Simulation results demonstrate that the proposed control strategy reduces computational complexity, improves operational efficiency, and enables real-time trajectory tracking.

The organization of this research is given as follows. A trajectory tracking model for UAVs was established in section II. In section III, the concept of MPC was utilized to transform the trajectory tracking problem into a constrained standard quadratic programming problem and considering the constraints imposed by UAV kinematics, the control increment constraints and relaxation factors was added in the objective function. The optimization performed by the dynamic neural network reduces computational complexity and improves operational efficiency. Additionally, we consider the presence of external disturbances and design disturbance compensation observers to overcome them. The effectiveness and stability of the proposed control strategy are validated through simulations. The conclusion and future work are presented in section VI.

## II. PROBLEM FORMULATION

Considering that the drone system consists of  $N$  UAVs flying at the same altitude, for the  $i$ th UAV, its dynamic characteristics can be described using a continuous-time mass-spring motion model as follows:

$$\begin{aligned}\dot{x}_i &= v_i \cos \theta_i \\ \dot{y}_i &= v_i \sin \theta_i \\ \dot{\theta}_i &= \omega_i\end{aligned}\quad (1)$$

where  $(x_i, y_i) \in R^2$  represents the position of the drone in the two-dimensional plane,  $\theta_i$  represents the heading angle,  $v_i$  and  $\omega_i$  represent the line speed and angular velocity of the drone.

The tracking process of the UAV trajectory is shown in Figure 1. The first UAV can perform real-time path planning through its onboard computer equipment, while other UAVs

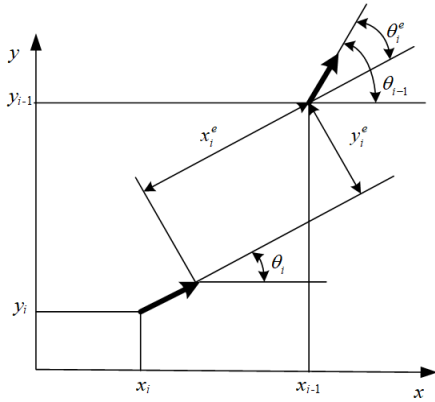


FIGURE 1. Diagram of UAV trajectory tracking.

track the previous UAV sequentially using their onboard positioning and sensor devices. They can obtain their own position and the position of the preceding UAV, and then calculate the relative distance between the two UAVs. The kinematic error of the  $i$ th UAV is described as follows:

$$\begin{cases} x_i^e = (x_{i-1} - x_i) \cos \theta_i + (y_{i-1} - y_i) \sin \theta_i \\ y_i^e = -(x_{i-1} - x_i) \sin \theta_i + (y_{i-1} - y_i) \cos \theta_i \\ \theta_i^e = -\theta_i + \theta_{i-1} \end{cases} \quad (2)$$

where  $x_i^e$  represents lateral tracking error,  $y_i^e$  represents longitudinal tracking error, and  $\theta_i^e$  represents the difference between the heading angle of  $i$ -th UAV and that of the previous UAV. Based on the error status and its kinematic model, the state equation of its kinematic error can be expressed as follows:

$$\begin{cases} \dot{x}_i^e = \omega_i y_i^e - v_i + v_{i-1} \cos \theta_i^e \\ \dot{y}_i^e = -\omega_i x_i^e + v_{i-1} \sin \theta_i^e \\ \dot{\theta}_i^e = -\omega_i + \omega_{i-1} \end{cases} \quad (3)$$

Furthermore, if  $\bar{x}_i^e = [\bar{x}_i^e, \bar{y}_i^e, \bar{\theta}_i^e]^T$  is defined, then the control signal is  $u_{i1} = v_{i-1} \cos \theta_i^e - v_i, u_{i2} = -\omega_i + \omega_{i-1}$ . The linear error state kinematic model is given as follows:

$$\dot{\bar{x}}_i^e = A_i \bar{x}_i^e + B_i u_i \quad (4)$$

where  $A_i = \begin{bmatrix} 0 & \omega_i & 0 \\ -\omega_i & 0 & v_{i-1} \\ 0 & 0 & 0 \end{bmatrix}, B_i = \begin{bmatrix} 1 & 0 \\ 0 & 0 \\ 0 & 1 \end{bmatrix}$ , and  $u_i = [u_{i1}, u_{i2}]^T$ .

Use the forward Euler method to discretize the linear error state kinematic model, and a more realistic model is given as,

$$\bar{x}_i^e(k+1) = \bar{A}_i \bar{x}_i^e(k) + \bar{B}_i u_i(k) + \bar{B}_i^d d_i(k) \quad (5)$$

where  $\bar{A}_i = (I + \tau A_i), \bar{B}_i = \tau B_i, \tau$  is the sampling time,  $B_i^d$  is the matrix of disturbance coefficients.

The objective of this research is to design a decentralized Model Predictive Control (MPC) for system (5) in order to solve the optimal decision variables of UAVs. This will enable the UAVs to accurately track desired trajectories in complex environments.

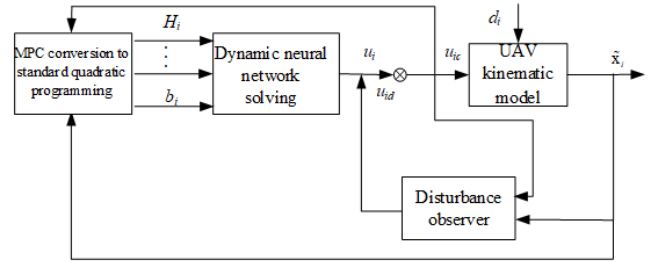


FIGURE 2. Tracking controller structure.

### III. DESIGN OF TRAJECTORY TRACKING CONTROLLER

When designing the trajectory tracking controller, external disturbances are taken into account. Therefore, the controller design for the  $i$ -th UAV is as follows:

$$u_{ic} = u_i + u_{id} \quad (6)$$

where the inputs of the MPC-based combined dynamic neural network controller is  $u_{ic}$  and the disturbance observer is  $u_{id}$ , and the control structure of UAV trajectory tracking is given in Figure 2.

#### A. MPC DESIGN

Model Predictive Control (MPC) algorithm transforms the optimization problem to be solved into a constrained quadratic cost function based on rolling time-domain. At each sampling moment, the estimated or measured model predictive system state information is used to ensure that the UAV quickly and smoothly tracks the required trajectory. The system state deviation and control vector optimization are considered in the controller. Then, using the predicted state information to optimize the defined objective function to obtain a series of control sequences, with the first quantity of the control sequence as the control input. Subsequently, repeated calculation at each subsequent sampling moment can obtain the desired control law. The objective function definition is shown below:

$$\begin{aligned} J_i(k) = & \sum_{j=1}^{N_p} y_i(k+j|k) - y_{i-1}(k+j|k)_{\bar{Q}}^2 \\ & + \sum_{j=1}^{N_c-1} \Delta u_i(k+j|k)_{\bar{R}}^2 + \rho \varepsilon^2(k) \end{aligned} \quad (7)$$

where the first term  $y_i(k+j|k)$  and  $y_{i-1}(k+j|k)$  represent the output states of the  $i$ th and  $(i-1)$ th UAV, which are used to evaluate the system's tracking performance. The second term  $\Delta u_i(k+j|k)$  represents the control increment of  $i$ th UAV.  $\|\cdot\|$  represents the Euclidean norm,  $\bar{Q}$  and  $\bar{R}$  are positive-definite matrices,  $N_p$  is the prediction time domain,  $N_c$  is the control time domain, and it satisfies  $N_p \geq N_c \geq 1$ .  $\varepsilon(k) = [\varepsilon_1(k) \ \varepsilon_2(k)]$  is a scaling factor that can ensure that the objective function always has a feasible solution.

In order to solve the objective function, a new variable is redefined:

$$\tilde{x}_i(k|k) = \begin{bmatrix} \tilde{x}_i^e(k|k) \\ u_i(k-1|k) \end{bmatrix} \quad (8)$$

Then, the corresponding matrix is transformed to obtain a new state space expression

$$\begin{aligned} \tilde{x}_i(k+1|k) &= \tilde{A}_i x_i(k|k) + \tilde{B}_i \Delta u_i(k|k) \\ y_i(k+1|k) &= \tilde{C}_i \tilde{x}_i(k+1|k) \end{aligned} \quad (9)$$

Subject to

$$\begin{aligned} u_{\min}(k) + \varepsilon_1(k)v_{1\min} &\leq u_i(k) \leq u_{\max}(k) + \varepsilon_1(k)v_{1\max} \\ \Delta u_{\min}(k) + \varepsilon_2(k)v_{2\min} &\leq \Delta u_i(k) \leq \Delta u_{\max}(k) + \varepsilon_2(k)v_{2\max} \\ \tilde{x}_{\min}(k) &\leq \tilde{x}_i(k) \leq \tilde{x}_{\max}(k) \end{aligned} \quad (10)$$

where  $\tilde{A}_i = \begin{bmatrix} \tilde{A}_i & \tilde{B}_i \\ 0_{m \times n} & I_m \end{bmatrix}$ ,  $\tilde{B}_i = \begin{bmatrix} \tilde{B}_i \\ I_m \end{bmatrix}$ ,  $\tilde{C}_i = [C_{1 \times n}, 0_{1 \times m}]$ .

$\Delta u_i(k) = u_i(k|k) - u_i(k-1|k)$ ,  $m$  represents the dimensionality of the state variables,  $n$  represents the dimensionality of the input control variables,  $v_{1\min}$  and  $v_{2\min}$  represent the lower bounds of the scaling factors, and  $v_{1\max}$  and  $v_{2\max}$  represent the upper bounds of the scaling factors.

At the current time  $k$ , the corresponding predicted state sequence is  $\tilde{x}_i(k+j|k)$ ,  $j = 1, 2, \dots, N_p$ , the output state can be obtained based on the previous moment  $\Delta u_i(k+j|k-1)$ ,  $j = 1, 2, \dots, N_c$  as,

$$\begin{aligned} y_i(k+1|k) &= \tilde{C}_i \tilde{A}_i \tilde{x}_i(k) + \tilde{C}_i \tilde{B}_i \Delta u_i(k) \\ y_i(k+2|k) &= \tilde{C}_i \tilde{A}_i^2 \tilde{x}_i(k) + \tilde{C}_i \tilde{A}_i \tilde{B}_i \Delta u_i(k) \\ &\quad + \tilde{C}_i \tilde{B}_i \Delta u_i(k+1|k) \\ &\vdots \\ y_i(k+N_p|k) &= \tilde{C}_i \tilde{A}_i^{N_p} \tilde{x}_i(k) + \tilde{C}_i \tilde{A}_i^{N_p-1} \tilde{B}_i \Delta u_i(k) + \dots \\ &\quad + \tilde{C}_i \tilde{A}_i^{N_p-N_c-1} \tilde{B}_i \Delta u_i(k+N_c-1|k) \end{aligned} \quad (11)$$

In order to simplify the expression, the prediction output is represented in matrix form:

$$Y_i(k) = \Phi_i(k) \tilde{x}_i(k|k) + \Theta_i(k) \Delta U_i(k) \quad (12)$$

$$\text{where } Y_i(k) = \begin{bmatrix} y_i(k+1|k) \\ y_i(k+2|k) \\ \vdots \\ y_i(k+N_p|k) \end{bmatrix}, \Phi_i(k) = \begin{bmatrix} \tilde{C}_i \tilde{A}_i \\ \tilde{C}_i \tilde{A}_i^2 \\ \vdots \\ \tilde{C}_i \tilde{A}_i^{N_p} \end{bmatrix}.$$

The prediction control increment matrices  $\Delta U_i(k) \in R^{mN_c}$  and  $\Theta_i(k) \in R^{mN_p \times mN_c}$  is given as follows:

$$\Delta U_i(k) = \begin{bmatrix} \Delta u_i(k|k) \\ \Delta u_i(k+1|k) \\ \vdots \\ \Delta u_i(k+N_c|k) \end{bmatrix},$$

$$\Theta_i(k) = \begin{bmatrix} \tilde{C}_i \tilde{B}_i & 0 & 0 & 0 \\ \tilde{C}_i \tilde{A}_i \tilde{B}_i & \tilde{C}_i \tilde{B}_i & 0 & 0 \\ \vdots & \vdots & \ddots & \vdots \\ \tilde{C}_i \tilde{A}_i^{N_p-1} \tilde{B}_i & \tilde{C}_i \tilde{A}_i^{N_p-2} \tilde{B}_i & \dots & \tilde{C}_i \tilde{B}_i \\ \tilde{C}_i \tilde{A}_i^{N_p} \tilde{B}_i & \tilde{C}_i \tilde{A}_i^{N_p-1} \tilde{B}_i & \dots & \tilde{C}_i \tilde{A}_i \tilde{B}_i \\ \vdots & \vdots & \ddots & \vdots \\ \tilde{C}_i \tilde{A}_i^{N_p-1} \tilde{B}_i & \tilde{C}_i \tilde{A}_i^{N_p-2} \tilde{B}_i & \dots & \tilde{C}_i \tilde{A}_i^{N_p-N_p-1} \tilde{B}_i \end{bmatrix}.$$

Then, the objective function of optimization can be written in the following form:

$$\min \Phi_i(k) \tilde{x}_i(k|k) + \Theta_i(k) \Delta U_i(k)_Q^2 + \Delta U_i(k)_R^2 + \varepsilon^T \rho \varepsilon \quad (13)$$

Subject to

$$\begin{aligned} \Delta U_{\min}(k) + \varepsilon_2(k)v_{2\min} &\leq \Delta U_i(k) \leq \Delta U_{\max}(k) + \varepsilon_2(k)v_{2\max} \\ U_{\min}(k) + \varepsilon_1(k)v_{1\min} &\leq U_i(k) + \tilde{I} \Delta U_i(k) \\ &\leq U_{\max}(k) + \varepsilon_1(k)v_{1\max} \\ Y_{\min}(k) &\leq Y(k) \leq Y_{\max}(k) \end{aligned} \quad (14)$$

$$\text{where } \tilde{I} = \begin{bmatrix} I & 0 & \dots & 0 \\ I & I & 0 & 0 \\ \vdots & \vdots & \ddots & \vdots \\ I & I & \dots & I \end{bmatrix} \in R^{mN_c \times mN_c}.$$

In order to facilitate the solution of dynamic neural networks, this optimization problem is further transformed into a standard quadratic programming problem as follow:

$$\min \begin{bmatrix} \Delta U_i(k) \\ \varepsilon(k) \end{bmatrix}^T W_i(k) \begin{bmatrix} \Delta U_i(k) \\ \varepsilon(k) \end{bmatrix} + b_i^T(k) \begin{bmatrix} \Delta U_i(k) \\ \varepsilon(k) \end{bmatrix} \quad (15)$$

Subject to

$$E_i \begin{bmatrix} \Delta U_i(k) \\ \varepsilon(k) \end{bmatrix} \leq c_i(k) \quad (16)$$

where

$$W_i(k) = \begin{bmatrix} \Theta_i(k)^T Q \Theta_i(k) + R & 0 \\ 0 & \rho \end{bmatrix},$$

$$b_i(k) = [M^T(k) Q \Theta_i(k) 0], M(k) = \Phi(k) \tilde{x}_i(k),$$

$$E_i = \begin{bmatrix} \tilde{I} & -V_{1\max} & 0 \\ -\tilde{I} & V_{1\min} & 0 \\ L & 0 & V_{2\max} \\ -L & 0 & V_{2\min} \end{bmatrix},$$

$$c_i(k) = \begin{bmatrix} U_{\max}(k) - U_i(k) \\ -U_{\min}(k) + U_i(k) \\ \Delta U_{\max}(k) \\ -\Delta U_{\min}(k) \end{bmatrix},$$

$$L = \begin{bmatrix} 1 & 0 & \dots & 0 \\ 0 & 1 & \dots & 0 \\ \vdots & \vdots & \ddots & \vdots \\ 0 & 0 & 0 & 1 \end{bmatrix} \in R^{mN_c \times mN_c}, U_{\max}$$

$$= \begin{bmatrix} u_{\max} \\ u_{\max} \\ \vdots \\ u_{\max} \end{bmatrix} \in \mathbf{R}^{mN_c}$$

with  $U_i(k) = 1_{N_c} \otimes u(k - 1)$ , where  $1_{N_c}$  represents the row vector of  $N_c$  rows with value 1,  $\otimes$  represents the Kronecker product. Defined  $\zeta_i(k) = [\Delta U_i(k) \ \varepsilon(k)]$ , the objective function can then be written in the following form:

$$\min \quad \zeta_i^T(k) W_i \zeta_i(k) + b_i^T(k) \zeta_i(k) \quad (17)$$

$$\text{s.t.} \quad E_i \zeta_i(k) \leq c_i(k) \quad (18)$$

In each control time domain, the control input increment can be calculated as

$$\Delta U_i^*(k) = [\Delta u_i^*(k) \ \Delta u_i^*(k + 1) \ \cdots \ \Delta u_i^*(k + N_c - 1)]$$

Finally, the control signal is applied to the system by taking the first element of the control column as

$$u_i(k) = u_i(k - 1) + \Delta u_i^*(k) \quad (19)$$

### B. DYNAMIC NEURAL NETWORK OPTIMIZATION DESIGN

In this subsection, a dynamic neural network is designed to solve real-time problems of standard quadratic programming with inequality constraints. The proposed network model considers decision vectors, equality constraints, and inequality constraints, resulting in a smaller network size compared to other neural network methods. Additionally, it does not require nonlinear operations such as matrix multiplication or inversion, making it easier to implement and reducing algorithm complexity, thus effectively improving the real-time performance of the algorithm. Furthermore, the activation function of the dynamic neural network based on linear variation inequality is piecewise linear and easy to implement, which can be used as a strategy for online.

Firstly, according to the duality theory, the primal quadratic programming problem can be solved by deriving it from its dual decision variables. Usually, the Lagrange multipliers of each constraint are defined as the dual decision variables. Therefore, we can define the dual decision variables  $\xi_i$  and its upper and lower bounds  $\xi_i^\pm$  as,

$$\xi_i = \begin{bmatrix} \zeta_i \\ \omega \end{bmatrix}, \xi_i^+ = \begin{bmatrix} \zeta_i^{\max} \\ +\omega^+ \end{bmatrix}, \xi_i^- = \begin{bmatrix} \zeta_i^{\min} \\ -\omega^- \end{bmatrix} \quad (20)$$

where  $\omega^\pm \geq 0$ , the dual decision variables satisfy the following inequalities

$$(\xi_i - \xi_i^*)^T (H_i \xi_i + p_i) \geq 0 \quad (21)$$

where  $H_i = \begin{bmatrix} W_i & -E_i^T \\ E_i^T & 0 \end{bmatrix}, p_i = \begin{bmatrix} c_i \\ -b_i \end{bmatrix}$ .

According to the duality theorem, the dual decision variables can be transformed into the following piecewise linear equalities

$$P_\Omega^i(\xi_i - (H_i \xi_i + q_i)) - \xi_i = 0 \quad (22)$$

The piecewise linear activation function  $P_\Omega^i(\cdot)$  is defined as follows,

$$P_\Omega^i(\xi_{ij}) = \begin{cases} \xi_{ij}^- & \text{if } \xi_{ij} < \xi_{ij}^- \\ \xi_{ij} & \text{if } \xi_{ij}^- \leq \xi_{ij} \leq \xi_{ij}^+ \\ \xi_{ij}^+ & \text{if } \xi_{ij} > \xi_{ij}^+ \end{cases}$$

In order to solve the piecewise linear equations and quadratic programming problems, we can refer to the neural network design experience in [25] and design the following neural network dynamics equation:

$$\dot{\xi}_i = \gamma (I + H_i^T) \{ P_\Omega^i(\xi_i - (H_i \xi_i + p_i)) - \xi_i \} \quad (23)$$

where  $\gamma$  is a dynamic parameter, typically a positive value, used to control the convergence speed of the neural network. A larger  $\gamma$  leads to faster convergence, but if  $\gamma$  is too large, it may cause convergence oscillations. The schematic diagram of the dynamic neural network structure is shown in Figure 3.

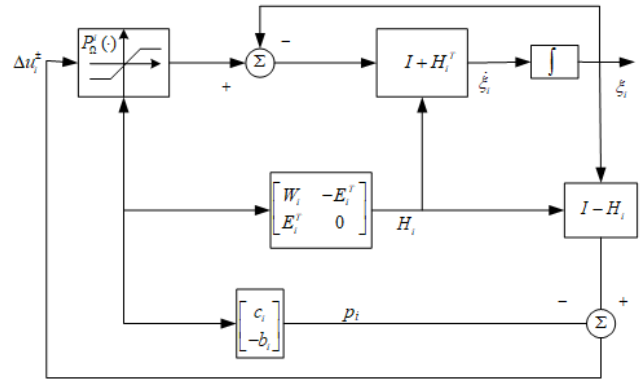


FIGURE 3. Block diagram of the dynamic neural network system.

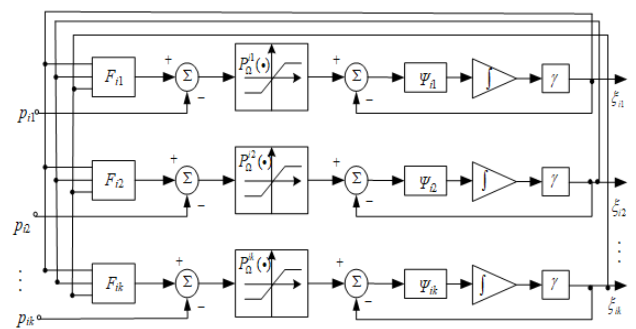


FIGURE 4. Structure of the neural network dynamic system.

After simple matrix and vector operations, the dynamic neural network can process quadratic programming problems in real-time and obtain the control input increment. As shown in Figure 4,  $\xi_i$  represents the output of the neural network corresponding to unmanned aerial vehicle  $i$ , and  $\Psi_{ik}$  represents the  $k$ th row element of matrix  $\psi_i = I + H_i^T$ . Assuming the dimension of the input vector is  $k$ , the network consists of  $k$  vector operation units,  $k$  projection operators,  $k$  adders, and  $k$  integrators.



**C. DESIGN OF DISTURBANCE COMPENSATION OBSERVER OF**

The previous UAV trajectory tracking method utilized model predictive control combined with dynamic neural network optimization for optimization. However, external disturbances were not taken into account. In this section, a composite trajectory tracking method is proposed that incorporates a disturbance compensation observer to suppress disturbances. Disturbances are considered in the error motion model

$$\dot{\bar{x}}_e^i(k+1) = \bar{A}_i \bar{x}_e^i(k) + \bar{B}_i u_i(k) + \bar{B}_d^i d_i(k) \quad (24)$$

According to [26], the disturbance compensation observer  $u_d^i$  can be designed as follows.

$$u_d^i = K_d^i \hat{d}_i \quad (25)$$

where  $\hat{d}_i$  represents the estimated value of disturbance  $d_i$ , and  $K_d^i$  is the disturbance compensation coefficient matrix, which can be calculated using the following equation,

$$(\bar{A}_i + \bar{B}_i K_x^i)^{-1} \bar{B}_d^i K_d^i = -(\bar{A}_i + \bar{B}_i K_x^i)^{-1} \bar{B}_d^i \quad (26)$$

where  $K_x^i$  is the feedback control coefficient matrix, and  $\hat{d}_i$  is computed as follows.

$$\hat{d}_i = z_i + L_i \bar{x}_i^e \quad (27)$$

$$\dot{z}_i = -L_i \bar{B}_d^i (z_i + L_i \bar{x}_i^e) - L_i (\bar{A}_i \bar{x}_i^e + \bar{B}_i u_i) \quad (28)$$

where  $z_i$  is the auxiliary vector and  $L_i$  is the observer coefficient matrix. The corresponding structure is shown in Figure 5.

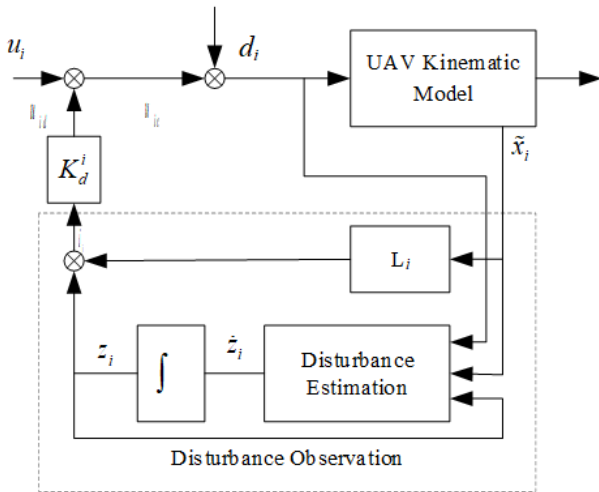


FIGURE 5. Disturbance observer.

In the kinematic error model, the inclusion of disturbances is represented as equation (23). In order to establish the stability of the closed-loop system, the following assumptions are made: the disturbances  $d_i(k)$  and  $\dot{d}_i(k)$  are bounded. Consequently, the disturbance estimation error  $e_d$  can be obtained as follows

$$e_{di} = \hat{d}_i(k) - d_i(k) \quad (29)$$

$$\begin{aligned} \dot{e}_d &= \dot{\hat{d}}_i(k) - \dot{d}_i(k) = \dot{z}_i + L_i \dot{\bar{x}}_i - \dot{d}_i(k) \\ &= -L \bar{B}_d^i \hat{d}_i(k) - L (\bar{A}_i \bar{x}_i + \bar{B}_i u_i) \\ &\quad + L (\bar{A}_i \bar{x}_i + \bar{B}_i u_i + \bar{B}_d^i d_i(k)) - \dot{d}_i(k) \\ &= -L \bar{B}_d^i e_{di} - \dot{d}_i(k) \end{aligned} \quad (30)$$

Finally, the proposed pseudocode for the UAV trajectory tracking algorithm combining model predictive control and neural networks is presented in Table 1.

TABLE 1. Model prediction combined with neural network of UAV tracking algorithm.

Input: UAV initial position, desired flight path
Output: UAV coordinated tracking trajectory
<ol style="list-style-type: none"> <li>1. Set <math>t=1</math>, total running time <math>T</math>, prediction horizon <math>Np</math>, control horizon <math>Nu</math>, sampling time <math>\tau</math>, and weighting coefficient matrices <math>Q</math> and <math>R</math>.</li> <li>2. Utilizing the established unmanned aerial vehicle trajectory tracking model, the problem is formulated as a quadratic programming problem using the MPC approach, aiming to determine the upper and lower bounds <math>\xi_{\min}, \xi_{\max}</math> for the dual decision variables in the dynamic neural network and matrix <math>W_i, E_i, c_i, b_i</math>.</li> <li>3. Utilizing the dynamic neural network, the quadratic programming problem for UAV<math>_i</math> is solved to obtain the optimal control input increment <math>\Delta u_i^*(k)</math>. The input <math>u_i(k+1)</math> is then calculated using equation (18).</li> <li>4. Considering the disturbance, the external disturbance is estimated using equations (26)-(27), and further, the compensation input <math>u_d^i</math> is calculated.</li> <li>5. The actual control input is obtained according to equation (6).</li> <li>6. If <math>t &lt; T</math>, increment <math>t</math> by 1 and proceed to step 2; otherwise.</li> <li>7. End.</li> </ol>

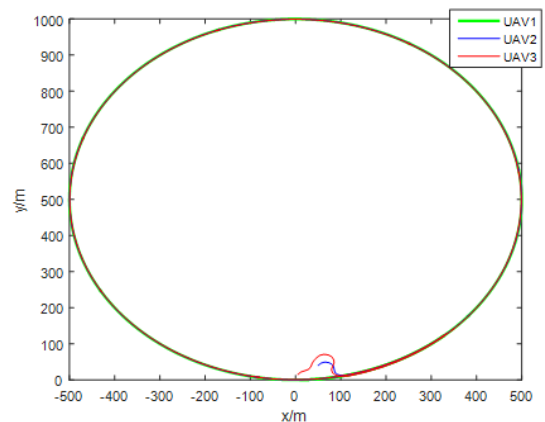


FIGURE 6. Tracking circle.

**IV. SIMULATIONS**

To verify the feasibility and accuracy of the proposed method in this paper, simulation analysis is conducted using Matlab

2015b on a PC device with an Intel Core i5-8400@2.80GHz processor and 8GB of memory. Firstly, the desired trajectory for the leader UAV is set as trajectory  $x_1 = 500 \cos(\theta_1)$ ,  $y_1 = 500 - 500 \cos(\theta_1)$ , with the initial position at the origin. Simulation analysis is then performed separately for two scenarios: without considering external disturbances and with the inclusion of external disturbances.

**A. WITHOUT CONSIDERING DISTURBANCES**

Next, simulation parameters are set, and the system constraints and their upper and lower bounds are defined. In this simulation, the running time is 200s, the sampling time is 500ms, the prediction horizon is denoted as  $N_p = 5$ , the control horizon is denoted as  $N_c = 5$ , the weight coefficient matrices are  $Q = 5I, R = I$  and  $\rho = \text{diag}\{1010\}$ , the upper and lower bounds of the control input are denoted as  $u_{\max} = [30, \pi/4]$  and  $u_{\min} = -u_{\max}$ , the upper and lower bounds of the input increment are denoted as  $\Delta u_{\max} = [5, \pi/10]$  and  $\Delta u_{\min} = -\Delta u_{\max}$ , and the upper and lower bounds of the scaling factor are denoted as  $v_{1 \max} = [0.5, 0.5], v_{1 \min} = -v_{1 \max}, v_{2 \max} = [0.1, 0.1], v_{2 \min} = -v_{2 \max}$ .

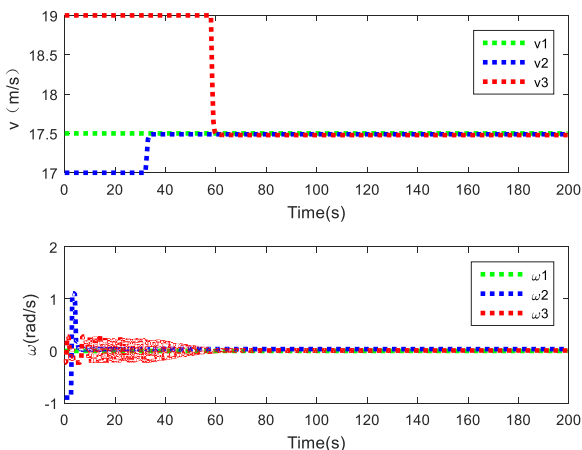


FIGURE 7. Control input without disturbance.

The results of tracking a circular trajectory without external disturbances are shown in Figure 6. In the figure, UAV1 represents the leader UAV following the designed trajectory, UAV<sub>2</sub> follows UAV<sub>1</sub>, and UAV<sub>3</sub> follows UAV<sub>2</sub>. It can be observed from the figure that the UAVs track the reference trajectory under the action of the controller and eventually maintain stable circular motion according to the reference trajectory. Figure 7 shows that after a certain period of time, the velocity control signals converge to stable values. The stable trajectory tracking can also be observed from Figure 8, where the state errors converge to zero. Figure 9 describes the instantaneous state of the neural network at any time  $k$ , and all the state variables of the neural network converge to the optimal solution within a short period of time. Next, we will further consider the trajectory tracking performance in the presence of external disturbances.

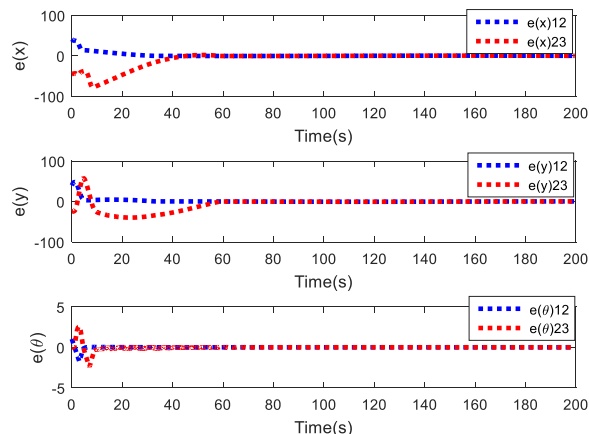


FIGURE 8. Tracking error without consider disturbance.

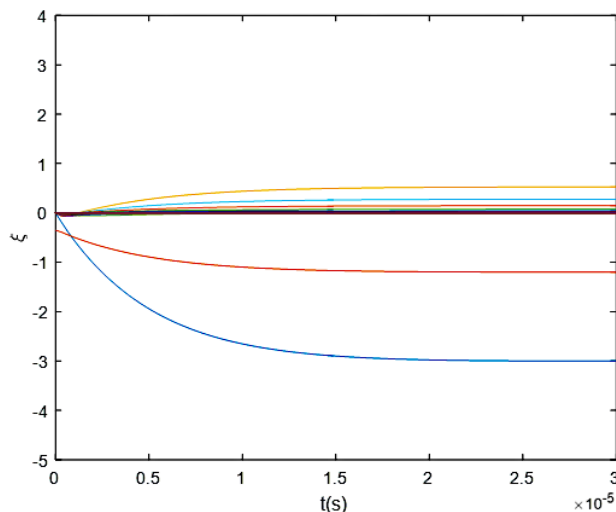


FIGURE 9. Convergent behaviors of the dynamic neural network.

**B. CONSIDERING DISTURBANCES**

In this simulation, the running time is 200s, the sampling time is 500ms, the prediction horizon is denoted as  $N_p = 5$ , the control horizon is denoted as  $N_c = 5$ , the weight coefficient matrices are denoted as  $Q = 5I, R = I$  and  $\rho = \text{diag}\{1010\}$ , the upper and lower bounds of the control input are denoted as  $u_{\max} = [30, \pi/4]$  and  $u_{\min} = -u_{\max}$ , the upper and lower bounds of the input increment are denoted as  $\Delta u_{\max} = [5, \pi/10]$  and  $\Delta u_{\min} = -\Delta u_{\max}$ , and the upper and lower bounds of the scaling factor are denoted as  $v_{1 \max} = [0.5, 0.5], v_{1 \min} = -v_{1 \max}, v_{2 \max} = [0.1, 0.1], v_{2 \min} = -v_{2 \max}$ . The upper and lower bounds of the disturbance are denoted as  $d_{\max} = \{0.10.1\}$  and  $d_{\min} = -d_{\max}$ . The coefficient matrices of the disturbance feedforward compensator are as follows,

$$B_d^i = \begin{bmatrix} 1 & 0 \\ 0 & 0 \\ 0 & 1 \end{bmatrix}, L_i = \begin{bmatrix} 1 & 0 & 0 \\ 0 & 0 & 1 \end{bmatrix}, K_d^i = \begin{bmatrix} -5 \\ -5 \\ -5 \end{bmatrix}.$$

The simulation results are shown in Figure 10. It illustrates the variations in linear and angular velocities of each UAV when considering external disturbances. Although the velocities of the following UAVs initially differ from the leading UAV, they eventually converge and closely match the velocity of the leading UAV after some time. Figure 11 displays the changes in the state variable errors of each UAV, demonstrating that the errors converge to zero eventually.

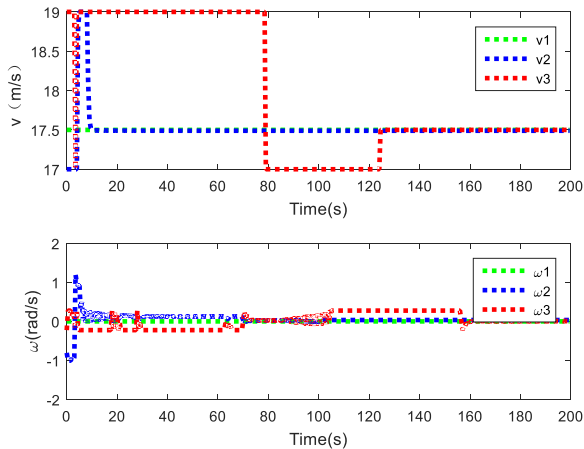


FIGURE 10. Control input with disturbance.

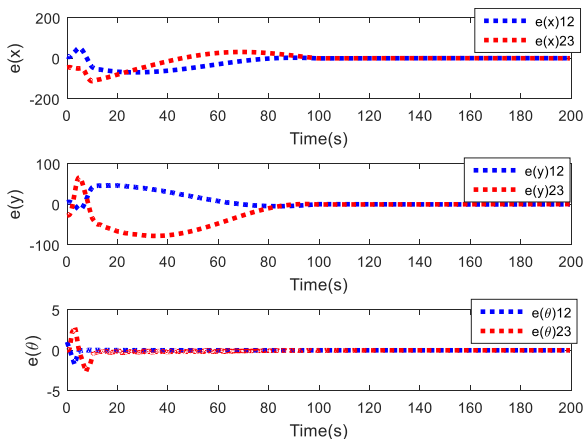


FIGURE 11. Control input with disturbance.

## V. CONCLUSION

This paper proposes a trajectory tracking control algorithm that combines model predictive control (MPC) with dynamic neural networks. The kinematic error model for UAV trajectory tracking is established, and the MPC concept is utilized to transform the trajectory tracking problem into a computationally tractable standard quadratic programming problem that can be solved online. Dynamic neural network methods are employed to solve this optimization problem within a limited rolling time horizon. Additionally, a disturbance feedforward compensation observer is designed to overcome the effects of external disturbances. Simulation

results demonstrate that this method reduces computational complexity, improves operational efficiency, and enables real-time UAV trajectory tracking.

## REFERENCES

- [1] Z. Lin, H. H. T. Liu, and M. Wotton, "Kalman filter-based large-scale wildfire monitoring with a system of UAVs," *IEEE Trans. Ind. Electron.*, vol. 66, no. 1, pp. 606–615, Jan. 2019.
- [2] J. Dong, K. Ota, and M. Dong, "UAV-based real-time survivor detection system in post-disaster search and rescue operations," *IEEE J. Miniat. Air Space Syst.*, vol. 2, no. 4, pp. 209–219, May 2021.
- [3] M. A. Lotufo, L. Colangelo, and C. Novara, "Control design for UAV quadrotors via embedded model control," *IEEE Trans. Control Syst. Technol.*, vol. 28, no. 5, pp. 1741–1756, Sep. 2020.
- [4] S. Bouabdallah and R. Siegwart, "Backstepping and sliding-mode techniques applied to an indoor micro quadrotor," in *Proc. IEEE Int. Conf. Robot. Autom.*, Apr. 2005, pp. 2247–2252.
- [5] S. Mobayen, F. F. M. El-Sousy, K. A. Alattas, O. Mofid, A. Fekih, and T. Rojsiraphisal, "Adaptive fast-reaching nonsingular terminal sliding mode tracking control for quadrotor UAVs subject to model uncertainties and external disturbances," *Ain Shams Eng. J.*, vol. 14, no. 8, Aug. 2023, Art. no. 102059.
- [6] A. Sir Elkhatem and S. Naci Engin, "Robust LQR and LQR-PI control strategies based on adaptive weighting matrix selection for a UAV position and attitude tracking control," *Alexandria Eng. J.*, vol. 61, no. 8, pp. 6275–6292, Aug. 2022.
- [7] L.-X. Xu, H.-J. Ma, D. Guo, A.-H. Xie, and D.-L. Song, "Backstepping sliding-mode and cascade active disturbance rejection control for a quadrotor UAV," *IEEE/ASME Trans. Mechatronics*, vol. 25, no. 6, pp. 2743–2753, Dec. 2020.
- [8] L. Wang and J. Su, "Trajectory tracking of vertical take-off and landing unmanned aerial vehicles based on disturbance rejection control," *IEEE/CAA J. Autom. Sinica*, vol. 2, no. 1, pp. 65–73, Jan. 2015.
- [9] X. Dong, Y. Li, C. Lu, G. Hu, Q. Li, and Z. Ren, "Time-varying formation tracking for UAV swarm systems with switching directed topologies," *IEEE Trans. Neural Netw. Learn. Syst.*, vol. 30, no. 12, pp. 3674–3685, Dec. 2019.
- [10] E. H. Zheng, J. J. Xiong, and I. L. Luo, "Second order sliding mode control for a quad rotor UAV," *ISA Trans.*, vol. 53, no. 4, pp. 1350–1356, 2014.
- [11] A. Parsa, S. B. Monfared, and A. Kalhor, "Backstepping control based on sliding mode for station-keeping of stratospheric airship," in *Proc. 6th RSI Int. Conf. Robot. Mechatronics (ICRoM)*, Oct. 2018, pp. 554–559.
- [12] H.-M. Wu, M. Karkoub, and C.-L. Hwang, "Mixed fuzzy sliding-mode tracking with backstepping formation control for multi-nonholonomic mobile robots subject to uncertainties," *J. Intell. Robot. Syst.*, vol. 79, no. 1, pp. 73–86, Jul. 2015.
- [13] C. Hui, C. Yousheng, and W. W. Shing, "Trajectory tracking and formation flight of autonomous UAVs in GPS-denied environments using onboard sensing," in *Proc. IEEE Chin. Guid., Navigat. Control Conf.*, Yantai, China, Aug. 2014, pp. 2639–2645.
- [14] Z. Zuo and S. Mallikarjunan, " $L_1$  adaptive backstepping for robust trajectory tracking of UAVs," *IEEE Trans. Ind. Electron.*, vol. 64, no. 4, pp. 2944–2954, Apr. 2017.
- [15] D. Invernizzi and M. Lovera, "Trajectory tracking control of thrust-vectoring UAVs," *Automatica*, vol. 95, pp. 180–186, Sep. 2018.
- [16] D. Invernizzi, M. Lovera, and L. Zaccarian, "Geometric trajectory tracking with attitude planner for vectored-thrust VTOL UAVs," in *Proc. Annu. Amer. Control Conf. (ACC)*, Milwaukee, WI, USA, Jun. 2018, pp. 3609–3614.
- [17] Z. Sun, H. Garcia de Marina, B. D. O. Anderson, and C. Yu, "Collaborative target-tracking control using multiple fixed-wing unmanned aerial vehicles with constant speeds," *J. Guid., Control, Dyn.*, vol. 44, no. 2, pp. 238–250, Feb. 2021.
- [18] H. Eslamiat, Y. Li, N. Wang, A. K. Sanyal, and Q. Qiu, "Autonomous waypoint planning, optimal trajectory generation and nonlinear tracking control for multi-rotor UAVs," in *Proc. 18th Eur. Control Conf. (ECC)*, Napoli, Italy, Jun. 2019, pp. 2695–2700.
- [19] J. B. Willis and R. W. Beard, "Pitch and thrust allocation for full-flight-regime control of winged eVTOL UAVs," *IEEE Control Syst. Lett.*, vol. 6, pp. 1058–1063, 2022, doi: 10.1109/LCSYS.2021.3089130.



[20] Y. Yang, L. Liao, H. Yang, and S. Li, "An optimal control strategy for multi-UAVs target tracking and cooperative competition," *IEEE/CAA J. Autom. Sinica*, vol. 8, no. 12, pp. 1931–1947, Dec. 2021.

[21] D. Invernizzi, M. Giurato, P. Gattazzo, and M. Lovera, "Comparison of control methods for trajectory tracking in fully actuated unmanned aerial vehicles," *IEEE Trans. Control Syst. Technol.*, vol. 29, no. 3, pp. 1147–1160, May 2021.

[22] Y. Mehmood, J. Aslam, N. Ullah, M. S. Chowdhury, K. Techato, and A. N. Alzaed, "Adaptive robust trajectory tracking control of multiple quad-rotor UAVs with parametric uncertainties and disturbances," *Sensors*, vol. 21, no. 7, p. 2401, Mar. 2021.

[23] B. S. Chen, Y. C. Liu, M. Y. Lee, and C. L. Hwang, "Decentralized H PID team formation tracking control of large-scale quadrotor UAVs under external disturbance and vortex coupling," *IEEE Access*, vol. 10, pp. 108169–108184, 2022.

[24] J. Wang, K. A. Alattas, Y. Bouteraa, O. Mofid, and S. Mobayen, "Adaptive finite-time backstepping control tracker for quadrotor UAV with model uncertainty and external disturbance," *Aerosp. Sci. Technol.*, vol. 133, Feb. 2023, Art. no. 108088.

[25] Y. Zhang, J. Wang, and Y. Xu, "A dual neural network for bi-criteria kinematic control of redundant manipulators," *IEEE Trans. Robot. Autom.*, vol. 18, no. 6, pp. 923–931, Dec. 2002.

[26] J. Yang, S. Li, and X. Yu, "Sliding-mode control for systems with mismatched uncertainties via a disturbance observer," *IEEE Trans. Ind. Electron.*, vol. 60, no. 1, pp. 160–169, Jan. 2013.



**LIGANG WU** was born in Datong, Shanxi, China, in 1986. He received the M.Sc. and Ph.D. degrees in control theory and control engineering from Dalian Maritime University, Dalian, China, in 2012 and 2016, respectively. He is currently an Associate Professor with the College of Mechanical and Electrical Engineering, Shanxi Datong University. His current research interests include machine learning algorithms, intelligent control and intelligent manufacturing, and other artificial intelligence fields.



**YUANYUAN LV** was born in Datong, Shanxi, China, in 1999. She received the B.E. degree in Internet of Things engineering from Taiyuan University, Taiyuan, in 2021. She is currently pursuing the degree in sources and environment with Shanxi Datong University. Her research interests include deep learning and object detection.



**LEI YANG** was born in Datong, Shanxi, China, in 1988. He received the master's degree in detection technology and automation device from Northwestern Polytechnical University, Xi'an, China, in 2015. He is currently a Lecturer with the College of Physical and Electronic Sciences, Shanxi Datong University. His current research interests include machine learning algorithms, fault diagnosis, and other artificial intelligence fields.



**ZHE ZHANG** was born in Xinzhou, Shanxi, China, in 1996. She received the B.E. degree in mathematics and applied mathematics from the Xi'an University of Finance and Economics, Xi'an, China, in 2017. She is currently pursuing the degree in source and environment. Her research interests include deep learning and object detection.

...